

Spectroscopic Evidence for Competing Reconstructions in Polar Multilayers LaAlO₃/LaVO₃/LaAlO₃

M. Takizawa,¹ Y. Hotta,² T. Susaki,² Y. Ishida,³ H. Wadati,¹ Y. Takata,^{3,4} K. Horiba,³ M. Matsunami,³ S. Shin,³
M. Yabashi,^{4,5} K. Tamasaku,⁴ Y. Nishino,⁴ T. Ishikawa,^{4,5} A. Fujimori,¹ and H. Y. Hwang^{2,6}

¹*Department of Physics, University of Tokyo, 3-7-1 Hongo, Bunkyo-ku, Tokyo, 113-0033, Japan*

²*Department of Advanced Materials Science, University of Tokyo, 5-1-5 Kashiwanoha, Kashiwashi, Chiba, 277-8651, Japan*

³*Excitation Order Research Team, RIKEN SPring-8 Center, Sayo-cho, Hyogo 679-5148, Japan*

⁴*Coherent X-ray Optics Laboratory, RIKEN SPring-8 Center, Sayo-cho, Hyogo 679-5148, Japan*

⁵*JASRI, SPring-8, Sayo-cho, Hyogo 679-5198, Japan*

⁶*Japan Science and Technology Agency, Kawaguchi, 332-0012, Japan*

(Received 8 June 2008; published 10 June 2009)

We have studied the valence redistribution of V in LaAlO₃/LaVO₃/LaAlO₃ trilayers, which are composed of only polar layers grown on SrTiO₃ (001) substrates, by core-level photoemission spectroscopy. We have found that the V valence is intermediate between V³⁺ and V⁴⁺ for thin LaAlO₃ cap layers, decreases with increasing cap-layer thickness, and finally recovers the bulk value of V³⁺ at ~10 unit-cell thickness. In order to interpret these results, we propose that the atomic reconstruction of the polar LaAlO₃ surface competes with the purely electronic V valence change so that the polar catastrophe is avoided at the cost of minimum energy.

DOI: 10.1103/PhysRevLett.102.236401

PACS numbers: 71.27.+a, 73.20.-r, 78.67.Pt, 79.60.Jv

Because of recent developments in oxide thin film fabrication, atomically controlled heterostructures of transition-metal oxides have become available and have attracted a great deal of attention from the fundamental physics as well as technological points of view [1–10]. For example, multilayers consisting of a band insulator SrTiO₃ and a Mott insulator LaTiO₃ exhibit metallic conductivity [1,2,8,11,12]. Interfaces between two band insulators, LaAlO₃ and SrTiO₃, also show metallic conductivity, and this interfacial conductivity depends on the termination layer [3]. That is, the (LaO)⁺/(TiO₂)⁰ interface is metallic, while the (AlO₂)⁻/(SrO)⁰ interface remains insulating, which implies that the polarity of the interface might be important for metallic transport. Remarkably, metallic transport at the LaAlO₃/SrTiO₃ interfaces occurs beyond a critical LaAlO₃ layer thickness of ~4–6 unit cells (uc) (~1.6–2.3 nm) [5,6]. In order to interpret such behavior, electronic reconstructions to avoid the polar catastrophe have been proposed [4,9,13,14]. In the (001) polar LaAlO₃, (LaO)⁺ and (AlO₂)⁻ are alternately stacked. A pair of positive and negative planes creates a dipole layer and the electrostatic potential divergently increases with the number of dipole layers. Since this situation is energetically unfavorable, some charge redistribution should occur. For the (LaO)⁺/(TiO₂)⁰ interface, the divergence can be avoided if half an electron ($-e/2$) is added to the interfacial region through the change of the Ti valence from Ti⁴⁺ to Ti^{3.5+}. Since electron-doped SrTiO₃ is metallic, this interface shows metallic conductivity. Meanwhile, for the (AlO₂)⁻/(SrO)⁰ interface, removing half an electron from the SrO layer can avoid the divergence. In this case, the oxygen vacancies are formed so that the interface remains insulating. On the other hand, some researchers

have argued that chemical imperfections such as oxygen vacancies are the origin of the metallic conductivity at the LaAlO₃/SrTiO₃ interface [15–17].

Given that both an electronic reconstruction as well as growth induced oxygen vacancies could explain the experimental results for the (LaO)⁺/(TiO₂)⁰ interface, it would be helpful to find a hole-doping analogue to this system, for which oxygen vacancies could be clearly ruled out as a mechanism. Recently, LaAlO₃/LaVO₃ multilayers, which are composed of only polar layers, have been fabricated and studied by photoemission spectroscopy (PES) [18–20]. It was found that the V 2*p* core-level spectra had not only V³⁺ components as expected from the chemical composition, but also a higher oxidation state V⁴⁺ component. Whether this V⁴⁺ component originated simply from chemical imperfections or some electronic reconstruction mechanism was unclear. In this work, we have performed a systematic LaAlO₃ cap-layer thickness dependence of the V valence in LaAlO₃/LaVO₃/LaAlO₃ trilayers using hard x-ray PES to probe deeply buried structures. We attribute this valence change to the competition between two types of reconstructions to avoid the polar catastrophe, namely, purely electronic V valence change and atomic reconstructions of the polar surface.

LaAlO₃(*x* uc)/LaVO₃(3 uc)/LaAlO₃(30 uc) trilayer samples, with varying LaAlO₃ cap-layer thickness *x*, were grown on the atomically flat, TiO₂-terminated (001) surface of SrTiO₃ substrates using pulsed laser deposition (PLD), as schematically shown in Fig. 1(a). All the trilayers were confirmed to be fully strained to the substrate by off-axis x-ray diffraction. The structures were grown at 600 °C under an oxygen partial pressure of 1×10^{-6} Torr, with a laser fluence of ~2 J/cm², following the previous

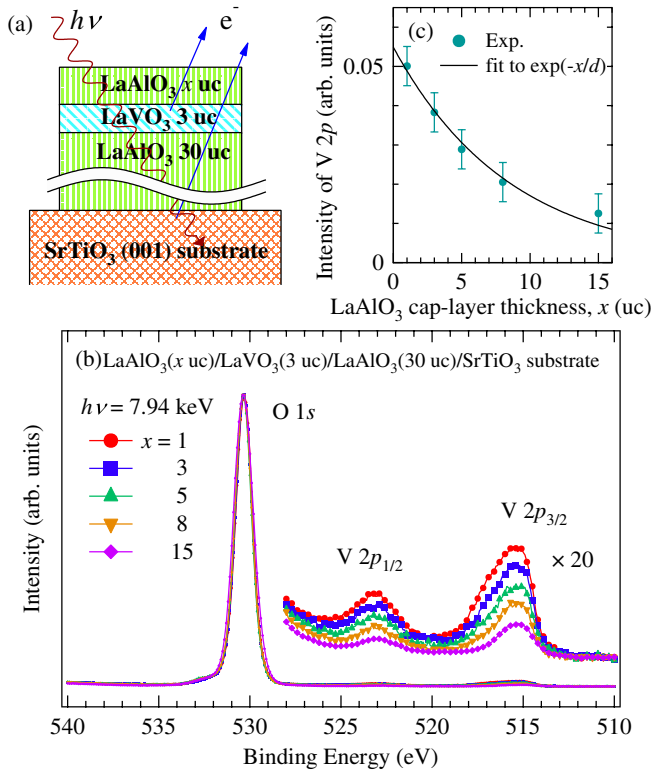


FIG. 1 (color online). Core-level spectra of the $\text{LaAlO}_3/\text{LaVO}_3/\text{LaAlO}_3$ trilayer samples. (a) Schematic view of the $\text{LaAlO}_3/\text{LaVO}_3/\text{LaAlO}_3$ trilayer samples grown on a SrTiO_3 (001) substrate. The LaAlO_3 cap-layer thickness was varied from 1 to 15 unit cells (uc) ($x = 1, \dots, 15$ uc). (b) O $1s$ and V $2p$ core-level spectra of the trilayer samples. (c) Intensity of the V $2p$ core level relative to that of the O $1s$ core level as a function of LaAlO_3 cap-layer thickness. The experimental data were well fitted to the function $a \exp(-x/d)$ where $d = 8.7 \pm 1$ uc.

optimization for two dimensional layer-by-layer growth of LaVO_3 [21]. Hard x-ray PES measurements were performed at the undulator beam line BL29XU of SPring-8, using a hemispherical electron energy analyzer, SCIENTA R4000-10 kV. Details of the apparatus including x-ray optics are described elsewhere [22–24]. Samples were transferred from the PLD chamber to the spectrometer chamber *ex situ*, and no surface treatment was performed prior to PES measurements. All the measurements were carried out at room temperature, and the total energy resolution was set to about 200 meV. The Fermi level (E_F) position was determined using gold spectra.

Figure 1(b) shows the O $1s$ and V $2p$ core-level spectra of the $\text{LaAlO}_3/\text{LaVO}_3/\text{LaAlO}_3$ trilayer samples with varying LaAlO_3 cap-layer thickness x , normalized to the O $1s$ peak height. Because the LaVO_3 layer was only 3 uc thick, the V $2p$ core-level signals were very small compared with those of O $1s$. Figure 1(c) shows the integrated intensity of the V $2p$ core level as a function of LaAlO_3 cap-layer thickness x . With increasing x , the intensity of the V $2p$ core level decreased, and the intensities were well

fitted to the exponential decay $a \exp(-x/d)$ with $d = 8.7 \pm 1$ uc ($\sim 3.5 \pm 0.4$ nm).

Figure 2(a) and 2(b) shows the V $1s$ and V $2p_{3/2}$ core-level spectra of the $\text{LaAlO}_3/\text{LaVO}_3/\text{LaAlO}_3$ trilayer samples and their line-shape analyses. In both spectra, one can clearly see two components. The low and high binding energy components can be assigned to V^{3+} and V^{4+} , respectively [25]. The V $1s$ and V $2p_{3/2}$ core-level spectra have therefore been decomposed into two features by line-shape analysis. With increasing LaAlO_3 cap-layer thickness, the structure on the higher binding-energy side (V^{4+}) decreases, meaning that as the LaVO_3 layer is more deeply buried in the LaAlO_3 environment, the V ion recovers the V^{3+} character of bulk LaVO_3 . In the line-shape analysis of the V $1s$ core-level spectra [Fig. 2(a)], an additional component from the La $2p$ core level located around ~ 5485 eV [20] has also been taken into account. For the line-shape analysis of the V $2p_{3/2}$ core-level spectra [Fig. 2(b)], three components were needed to reproduce the experimental results well. One feature located around ~ 517 eV is the V^{4+} component, and two other features located around ~ 515 eV and ~ 516 eV represent the multiplet structure of the V^{3+} component, as confirmed by cluster-model calculations including atomic multiplet structure. Figure 2(c) shows the resulting V^{3+} intensity relative to the total V intensity as a function of LaAlO_3 cap-layer thickness. With increasing thickness, the V^{3+} component increases and saturates toward ~ 1.0 beyond ~ 10 uc.

Let us propose the possible scenario for the origin of the present observations, together with the previous report that the valence distribution of V was highly asymmetric in the

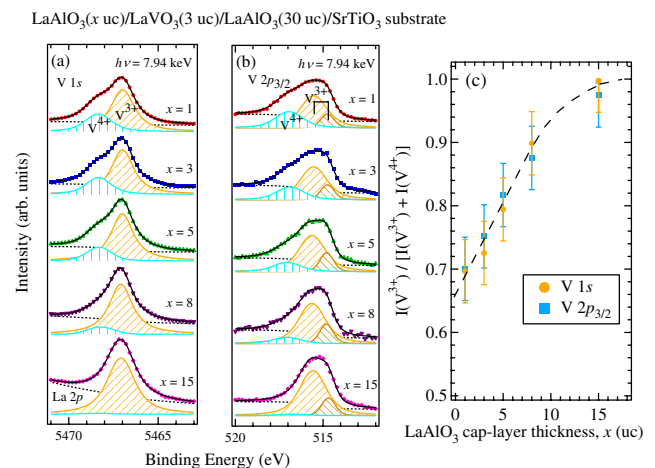


FIG. 2 (color online). LaAlO_3 cap-layer thickness dependence of the V core-level spectra of the $\text{LaAlO}_3(x \text{ uc})/\text{LaVO}_3(3 \text{ uc})/\text{LaAlO}_3(30 \text{ uc})$ trilayer samples grown on SrTiO_3 substrates. (a) V $1s$ core-level spectra and their line-shape analyses. (b) V $2p_{3/2}$ core-level spectra and their line-shape analyses. (c) LaAlO_3 cap-layer thickness dependence of the V^{3+} intensity relative to the total V intensity ($\text{V}^{3+} + \text{V}^{4+}$) in the V $1s$ and $2p_{3/2}$ core-level spectra. The dashed curve is a guide to the eye.

LaVO₃ layers in LaAlO₃/LaVO₃/LaAlO₃ [18,20]. That is, V⁴⁺ was preferentially distributed on the top side of the LaVO₃ layers. These features can be explained by considering the electrostatic potential of the trilayer, as schematically shown in Fig. 3. If all of the constituent materials preserve their bulk electronic and atomic configurations, the LaAlO₃/LaVO₃/LaAlO₃ trilayer films would consist of only polar planes and suffer from the polar catastrophe as shown in Fig. 3(a). In order to avoid this, two types of reconstructions that dramatically alter the electrostatic potential may be possible. In the first process [Fig. 3(b)], the polar (AlO₂)⁻ surface of LaAlO₃ is reconstructed [26,27], resulting in the net ejection of the charge $-e/2$. Therefore, the LaVO₃ layer is not affected. In the alternative process [Fig. 3(c)], the valence of the V ion changes from V³⁺ to V^{3.5+} and thereby $-e/2$ is removed from the top side of the embedded LaVO₃ layer. Note, however, that the precise determination of net charge transfer is impossible because it depends on the definition of the interface region, and the net charge transfer is not necessarily equal to $-e/2$ in real systems, as experimentally observed in Ref. [4].

Between the two types of reconstructions, the energetically more favorable one will be realized for a given LaAlO₃ cap-layer thickness. When the LaAlO₃ cap-layer thickness is thin, the electrostatic potential within the LaAlO₃ cap layer is small and the valence change V³⁺ →

V⁴⁺ occurs [Fig. 3(c)]. As the LaAlO₃ cap layers become thicker, the potential within the top LaAlO₃ cap layers grows in proportion to the LaAlO₃ cap-layer thickness, and this increasing energy cost becomes too large to be compensated by the valence change of V. Then, the reconstruction of the LaAlO₃ surface would become most effective to suppress the potential divergence of the entire trilayer and the valence change of V becomes unnecessary. Thus, the valence state of V in the LaVO₃ layers returns to its original bulklike value of V³⁺ [Fig. 3(b)]. Consequently, the observed V valence change with LaAlO₃ cap-layer thickness [Fig. 2(c)] can be considered as the result of these two competing processes. Although a surface reconstruction evolving with the LaAlO₃ cap-layer thickness was not directly probed in this experiment, the surface reconstruction should occur for the thick LaAlO₃ cap-layer thickness as in the case of LaAlO₃ single crystals [26,27]. It should be noted that such a thickness dependence of the V valence cannot be due to oxidation through the sample surface, because transport properties of LaAlO₃(x uc)/LaVO₃(3 uc)/LaAlO₃(substrate) structures were unaffected by the presence or absence of an additional 10 uc SrTiO₃ layer deposited on top [28]. The removed electron is effectively transferred to the SrTiO₃ substrate in either process (Fig. 3). These transferred electrons can be seen as an additional Ti³⁺ component from the film-substrate interface of the LaAlO₃/LaVO₃/LaAlO₃ trilayer sample as shown in Fig. 4. Despite the 38 uc thickness of the trilayer, the Ti signals from the SrTiO₃ substrate were clearly observed due to the long electron escape depth of hard x-ray PES.

Finally, it is worth remarking on the relationship between the present observations and the thickness dependence of the interface carrier density in LaAlO₃/SrTiO₃

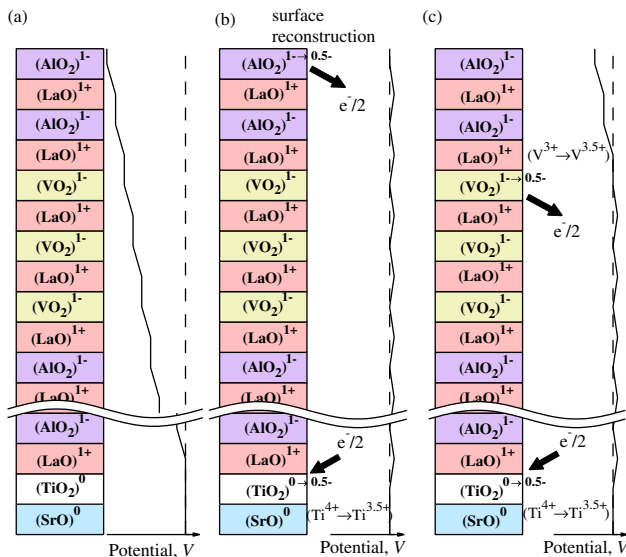


FIG. 3 (color online). Schematic illustrations of the reconstructions resolving the polar catastrophe in the all polar LaAlO₃/LaVO₃/LaAlO₃ trilayers. (a) The structures with all polar planes suffer from a polar catastrophe. (b) The top surface of LaAlO₃ undergoes the usual atomic reconstruction, whereas the bottom LaAlO₃/SrTiO₃ interface accepts the extra electrons through the electronic reconstruction Ti⁴⁺ → Ti^{3.5+}, thereby providing a compensating dipole. (c) Alternatively, the valence change (V³⁺ → V^{3.5+}) can also create extra electrons, resulting in purely electronic reconstructions on both sides of the trilayer. In the limit of a thick top LaAlO₃ layer, process (b) overcomes process (c).

LaAlO₃(5 uc)/LaVO₃(3 uc)/LaAlO₃(30 uc)/SrTiO₃ substrate

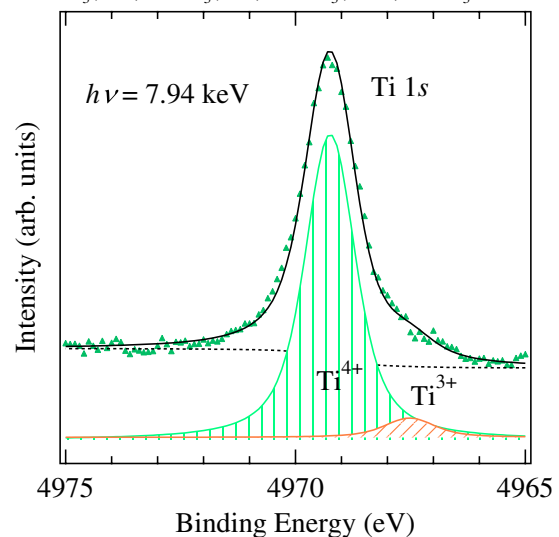


FIG. 4 (color online). Typical Ti 1s core-level spectrum of the LaAlO₃(5 uc)/LaVO₃(3 uc)/LaAlO₃(30 uc) trilayer grown on an SrTiO₃ substrate.

heterostructures, showing a critical LaAlO_3 layer thickness of 4–6 uc [5,6]. This behavior may also be interpreted in the same scenario: For thin LaAlO_3 layer thickness, the electrostatic potential within the LaAlO_3 layer remains small, and therefore the redistribution of charges does not have to occur. With increasing LaAlO_3 thickness, reconstruction of the LaAlO_3 surface donates charges $-e/2$ to the interfacial region, inducing carriers on the SrTiO_3 side. While electrons are induced at the interface of $\text{LaAlO}_3/\text{SrTiO}_3$, we have demonstrated hole-doping into the interface by designing the polar $\text{LaAlO}_3/\text{LaVO}_3/\text{LaAlO}_3$ trilayers. This technique should be quite general, so long as electronic reconstructions become energetically favorable to surface reconstructions. These results, together with previous studies on $\text{LaAlO}_3/\text{SrTiO}_3$, demonstrate that both positive and negative charge injection at heterointerfaces are feasible, opening a new route to the materials science and engineering of transition metal oxides.

In conclusion, we have performed a hard x-ray photoemission spectroscopy study on the $\text{LaAlO}_3/\text{LaVO}_3/\text{LaAlO}_3$ trilayers. The V core-level spectra showed two components, which we assigned to V^{3+} and V^{4+} valence states. The intensity of the V^{3+} component increased with LaAlO_3 cap-layer thickness and saturated beyond $\gg 10$ unit cells. This behavior can be explained by competing electronic reconstructions. This work demonstrates the feasibility to artificially hole-dope oxide heterostructures by atomic control of the electrostatic boundary conditions.

We thank D. A. Muller and G. A. Sawatzky for fruitful discussions. This work was supported by a Grant-in-Aid for Scientific Research (A19204037) from the Japan Society for the Promotion of Science and a Grant-in-Aid for Scientific Research in Priority Areas “Invention of Anomalous Quantum Materials” from the Ministry of Education, Culture, Sports, Science and Technology. M. T. acknowledges support from the Japan Society for the Promotion of Science for Young Scientists.

-
- [1] A. Ohtomo, D. A. Muller, J.L. Grazul, and H. Y. Hwang, *Nature (London)* **419**, 378 (2002).
- [2] S. Okamoto and A.J. Millis, *Nature (London)* **428**, 630 (2004).
- [3] A. Ohtomo and H. Y. Hwang, *Nature (London)* **427**, 423 (2004).
- [4] N. Nakagawa, H. Y. Hwang, and D. A. Muller, *Nature Mater.* **5**, 204 (2006).
- [5] M. Huijben, G. Rijnders, D. A. Muller, S. Bals, S. Van Aert, J. Verbeeck, G. Van Tendeloo, A. Brinkman, and H. Hilgenkamp, *Nature Mater.* **5**, 556 (2006).
- [6] S. Thiel, G. Hammeri, A. Schmehl, C. W. Schneider, and J. Mannhart, *Science* **313**, 1942 (2006).
- [7] A. Brinkman, M. Huijben, M. Van Zalk, J. Huijben, U. Zeiter, J.C. Maan, W.G. Van der Wiel, G. Rijnders, D.H.A. Blank, and H. Hilgenkamp, *Nature Mater.* **6**, 493 (2007).
- [8] R. Pentcheva and W.E. Pickett, *Phys. Rev. Lett.* **99**, 016802 (2007).
- [9] W.-C. Lee and A. H. MacDonald, *Phys. Rev. B* **76**, 075339 (2007).
- [10] N. Reyren, S. Thiel, A. D. Caviglia, L. Fitting Kourkoutis, G. Hammert, C. Richter, C. W. Schneider, T. Kopp, A.-S. Rüetschi, D. Jaccard, M. Gabay, D. A. Muller, J.-M. Triscone, and J. Mannhart, *Science* **317**, 1196 (2007).
- [11] K. Shibuya, T. Ohnishi, M. Kawasaki, H. Koinuma, and M. Lippmaa, *Jpn. J. Appl. Phys.* **43**, L1178 (2004).
- [12] M. Takizawa, H. Wadati, K. Tanaka, M. Hashimoto, T. Yoshida, A. Fujimori, A. Chikamatsu, H. Kumigashira, M. Oshima, K. Shibuya, T. Mihara, T. Ohnishi, M. Lippmaa, M. Kawasaki, H. Koinuma, S. Okamoto, and A. J. Millis, *Phys. Rev. Lett.* **97**, 057601 (2006).
- [13] R. Hesper, L. H. Tjeng, A. Heeres, and G. A. Sawatzky, *Phys. Rev. B* **62**, 16046 (2000).
- [14] C. Noguera, *J. Phys. Condens. Matter* **12**, R367 (2000).
- [15] A. Kalabukhov, R. Gunnarsson, J. Börjesson, E. Olsson, T. Claeson, and D. Winkler, *Phys. Rev. B* **75**, 121404(R) (2007).
- [16] W. Siemons, G. Koster, H. Yamamoto, W. A. Harrison, G. Lucovsky, T.H. Geballe, D.H.A. Blank, and M.R. Beasley, *Phys. Rev. Lett.* **98**, 196802 (2007).
- [17] G. Herranz, M. Basletić, M. Bibes, C. Carrétéro, E. Tafrá, E. Jacquet, K. Bouzehouane, C. Deranlot, A. Hamzić, J.-M. Broto, A. Barthélémy, and A. Fert, *Phys. Rev. Lett.* **98**, 216803 (2007).
- [18] Y. Hotta, H. Wadati, A. Fujimori, T. Susaki, and H. Y. Hwang, *Appl. Phys. Lett.* **89**, 251916 (2006).
- [19] H. Wadati, Y. Hotta, M. Takizawa, A. Fujimori, T. Susaki, and H. Y. Hwang, *J. Appl. Phys.* **102**, 053707 (2007).
- [20] H. Wadati, Y. Hotta, A. Fujimori, T. Susaki, H. Y. Hwang, Y. Takata, K. Horiba, M. Matsunami, S. Shin, M. Yabashi, K. Tamasaku, Y. Nishino, and T. Ishikawa, *Phys. Rev. B* **77**, 045122 (2008).
- [21] Y. Hotta, Y. Mukunoki, T. Susaki, H. Y. Hwang, L. Fitting, and D. A. Muller, *Appl. Phys. Lett.* **89**, 031918 (2006).
- [22] Y. Takata, M. Yabashi, K. Tamasaku, Y. Nishino, D. Miwa, T. Ishikawa, E. Ikenaga, K. Horiba, S. Shin, M. Arita, K. Shimada, H. Namatame, M. Taniguchi, H. Nohira, T. Hattori, S. Södergren, B. Wannberg, and K. Kobayashi, *Nucl. Instrum. Methods Phys. Res., Sect. A* **547**, 50 (2005).
- [23] K. Tamasaku, Y. Tanaka, M. Yabashi, H. Yamazaki, N. Kawamura, M. Suzuki, and T. Ishikawa, *Nucl. Instrum. Methods Phys. Res., Sect. A* **467–468**, 686 (2001).
- [24] T. Ishikawa, K. Tamasaku, and M. Yabashi, *Nucl. Instrum. Methods Phys. Res., Sect. A* **547**, 42 (2005).
- [25] K. Maiti and D.D. Sarma, *Phys. Rev. B* **61**, 2525 (2000).
- [26] R. J. Francis, S. C. Moss, and A. J. Jacobson, *Phys. Rev. B* **64**, 235425 (2001).
- [27] C.H. Lanier, J.M. Rondinelli, B. Deng, R. Kilaas, K. R. Poeppelmeier, and L.D. Marks, *Phys. Rev. Lett.* **98**, 086102 (2007).
- [28] T. Higuchi, Y. Hotta, T. Susaki, A. Fujimori, and H. Y. Hwang, *Phys. Rev. B* **79**, 075415 (2009).